Ultrasonics 54 (2014) 684–693

Contents lists available at ScienceDirect

Ultrasonics

journal homepage: www.elsevier.com/locate/ultras

Noncollinear wave mixing for measurement of dynamic processes in polymers: Physical ageing in thermoplastics and epoxy cure

A. Demčenko [a,*], V. Koissin [a], V.A. Korneev [b]

[a] Faculty of Engineering Technology, University of Twente, 7500AE Enschede, The Netherlands
[b] Lawrence Berkeley National Laboratory, Berkeley, California, United States

ARTICLE INFO

Article history:
Received 21 February 2013
Received in revised form 4 September 2013
Accepted 6 September 2013
Available online 15 September 2013

Keywords:
Non-linear ultrasonics
Physical ageing
Epoxy cure
Rheometry

ABSTRACT

Elastic wave mixing using an immersion method has shown effective monitoring and scanning capabilities when applied to thermoplastic ageing, epoxy curing, and non-destructive testing. In water, excitation and reception of waves do not require physical contact between the tools and the specimen, making the acquisition of high-resolution C-scans possible. The nonlinear material parameters exhibit a much higher sensitivity to the specimen state compared to linear ones. Thus, the nonlinear data for polymethyl methacrylate (PMMA) have a 40% difference between zones of "young" and "aged" material, while the linear data show no difference at all. Methodology and logistics of the immersion wave-mixing method are discussed in detail. Monitoring of epoxy curing has also revealed a good sensitivity of the method to this complex process including several characteristic stages, such as the time of maximal viscosity, the gel time, and the vitrification time. These stages are independently verified in separate rheometry measurements. The presented method allows for a number of possibilities: wave-mode and frequency separations, elimination of surrounding medium influence, "steering" (scanning) a scattered wave, controlling the location of the intersection volume, single-sided or double-sided measurements, and operation in detector mode.

1. Introduction

Elastic wave mixing can be used for nondestructive material testing and monitoring. This possibility has emerged after an immersion method was introduced recently in which an entire measurement assembly is immersed in a water tub [1–3]. In water, excitation and reception of waves occur without requiring physical contact between the tools and the specimen, making possible the acquisition of high-resolution C-scans [2]. The importance of the wave-mixing method is emphasized by observations, reported in this paper, showing that nonlinear material parameters have a higher sensitivity to the specimen state compared to linear parameters. In keeping with these observations, we show that the detection of the physical ageing of thermoplastics [1,4,5] and epoxy curing, e.g. [6–8], is higher when a nonlinear wave-mixing method is used.

Elastic nonlinearity of different materials, including rock samples, has been observed for ultrasonic frequencies by many authors [9–18]. In particular, it has been shown that the velocity of elastic waves changes with static deformation and hydrostatic pressure. This phenomenon, known as acousto-elasticity, is widely used for measurements of third-order elastic constants in solids. Waves of mixed frequencies as a result of nonlinear wave interaction have also been reported [19–22]. The fundamental equations of nonlinear elastic theory, by Murnaghan [23], effectively describe such classical nonlinear phenomena as harmonics generation and resonant wave scattering.

This paper presents experimental noncollinear wave mixing for testing of polymers, and it is structured as follows: The opening two sections are devoted to the logistics of the immersion wave-mixing method, describing a hierarchy of observation-parameter choices and various tradeoffs. Then, the aging process is studied in two examples of thermoplastics: polymethyl methacrylate (PMMA) and polyvinyl chloride (PVC). Changes in these materials were monitored after erasing a previous thermo-history of the polymer by heating. In other experiments, some, but not all, of the thermoplastic samples were rejuvenated and then scanned using linear and nonlinear techniques, revealing pronounced transition zones. Then we describe the monitoring of epoxy curing at two different temperatures—a complex process with several characteristic stages. This monitoring allowed us to detect these stages, which were verified in separate rheometry measurements. In the last experiment, we obtain a C-scan of an epoxy layer cured between two aluminium plates with naturally formed bubbles. The obtained nonlinear image is found to have comparable information to the information obtained by the linear ultrasonics technique.

* Corresponding author. +370 65444101.
E-mail address: andriejus.demcenko@gmail.com (A. Demčenko).

0041-624X/$ - see front matter © 2013 Elsevier B.V. All rights reserved.
http://dx.doi.org/10.1016/j.ultras.2013.09.011

2. Noncollinear wave mixing

In isotropic nonlinear materials, described by the third order elastic constants *l, m, n* or *A, B, C* [24], where can exist the *resonant conditions* when two elastic waves can interact to generate scattered waves with mixed (sum and difference) frequencies. The equations

$$\omega_r = \omega_1 \pm \omega_2 \tag{1}$$

$$\mathbf{k}_r = \mathbf{k}_1 \pm \mathbf{k}_2 \tag{2}$$

express these conditions, where frequencies ω_1, ω_2 and ω_r respectively represent two initial waves and a resonant wave, and $\mathbf{k}_1$, $\mathbf{k}_2$, and $\mathbf{k}_r$ are their wave vectors. Even if the resonant conditions were satisfied, the amplitude of the scattered wave might be zero for all parameter combinations (polarization restriction). In Korneev et al. [24] it is shown that only 10 out of 54 possible combinations of compressional L, shear SV, and shear SH waves generate scattered waves. Among the allowed combinations, two of them are collinear, meaning that the two primary waves propagate in the same direction. Use of collinear waves for material testing is limited, because it is technically difficult to generate them in an independent manner. Interaction of waves propagating in exactly opposite directions is possible for seven wave combinations [24].

There are several reasons to use noncollinear wave mixing for testing of materials. First, as will be shown below, some nonlinear material properties can be much more sensitive to changes caused by variations in temperature, aging, solidification etc., when compared to the corresponding linear properties. Second, the nonlinear resonant scattered waves can be easily extracted from the total wave field by narrow-band filtering, because the target and initial wave frequencies are different and pre-chosen. Third, the wave-mixing conditions allow convenient placement of transducers in different nonconflicting locations, making the entire installation easy to assemble and operate.

In the first wave-mixing measurements [15,16], the wave resonant conditions (interaction and scattering angles) were satisfied by preparing the specimens with a special geometry in which emitting as well as receiving transducers were glued to the specimen's sides. This kind of measurement technique requires a laborious preparation and is not flexible to changes in the model (wave propagation velocities) or observation (angles and frequencies) parameters. Some recently developed methods [1–3] with both submerged specimens and transducers are nondestructive and assume no physical contact between the specimen and measurement devices. Fig. 1 shows a submerged wave-mixing technique scheme with two modifications, using either reflected or transmitted scattered waves. For thick objects, the transmitted

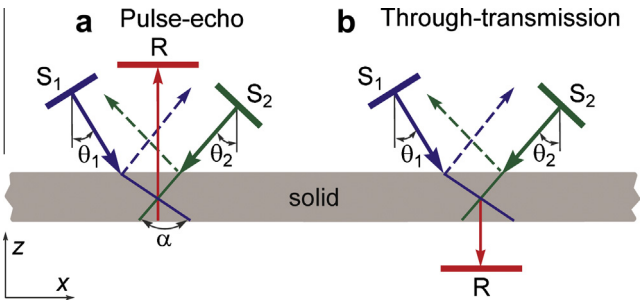

Fig. 1. Pulse-echo and through-transmission arrangement of transducers for single-side (a) and double-side (b) access measurements. Shown are the scattered wave receiver R, the pump wave sources $S_{1,2}$ having inclination angles $\theta_{1,2}$. Red lines show propagation paths of the resonant wave. Dashed lines mark the specularly reflected pump waves. α is the interaction angle between the two pump waves.

wave might be preferred, because the target scattered wave has a shorter path (less attenuation) and can be better detected. The advantage of the reflected wave scheme is in single-side-access to the specimen.

Knowing the longitudinal and shear wave velocities in the specimen, we can compute the incident angles of the sample boundary for the pump waves from the resonant conditions, also taking into account the angles of refraction on the water and specimen interface. We choose the sets of initial frequencies and angles to generate the propagation of scattered waves perpendicular to the interface, providing a maximum detectable signal above or below the specimen. When the specimen is thick and the source angles are inaccurately chosen, there is the risk that the scattered wave signal will deflect significantly from where the wave would be expected to propagate. This deflection is stronger in single-side-access measurements. Use of long, monochromatic primary signals ensures narrow spectral peaks for the recorded traces and robust detection of the scattered wave. The long signals also enable a certain misalignment of the pump wave sources in the vertical axis *z* (see Fig. 1). The choice of primary frequencies should also allow easy separation of the mixed frequencies from the primary waves and their multiples.

For the submerged wave mixing, the most interesting interactions are

(1) $\mathrm{SV}(\omega_1) + \mathrm{L}(\omega_2) \rightarrow \mathrm{L}(\omega_1 + \omega_2)$;
(2) $\mathrm{SV}(\omega_1) + \mathrm{SV}(\omega_2) \rightarrow \mathrm{L}(\omega_1 + \omega_2)$,

in which SV and L are the in-plane shear and longitudinal waves, respectively. The corresponding nonlinear wave amplitude coefficients (with dimension $length^{-3}$) are [24]:

$$W_1 = \frac{D_L}{2\gamma^3}\frac{\sin\alpha}{1+d}[C_1(3d\gamma+2q)+C_2q+C_3(d\gamma+q)+C_5d\gamma] \approx \frac{D_L}{2\gamma^3}\frac{\sin\alpha}{1+d}(d\gamma+q)m, \tag{3}$$

$$W_2 = D_L\frac{1+d}{2\gamma^2}[C_1\cos 2\alpha + C_2\cos^2\alpha - C_3\sin^2\alpha] \approx D_L\frac{1+d}{2\gamma^2}m\cos 2\alpha, \tag{4}$$

where the following notations are used

$$q = \cos\alpha(2d\gamma\cos\alpha + 1 + 2\gamma^2d^2), \tag{5}$$

$$D_L = d/(4\pi c_L^2\rho)(\omega_1/c_r)^3, \tag{6}$$

$$\gamma = c_S/c_L, \tag{7}$$

$$d = \omega_2/\omega_1. \tag{8}$$

Parameter α is the wave interaction angle (see Fig. 1a), c_L and c_S are the longitudinal and shear wave velocities in a medium, respectively, ρ is the material density, c_r is the nonlinear wave velocity in a medium and in our case $c_r = c_L$. The constants C_i have simple relations

$$C_1 = \mu + \frac{A}{4},\ C_2 = \lambda + \mu + \frac{A}{4} + B,\ C_3 = \frac{A}{4} + B,\ C_4 = B + 2C,\ C_5 = \lambda + B, \tag{9}$$

with third order elastic constants and Lamé parameters λ and μ.

Both of the interactions considered here can be used in single-sided or double-sided-access measurement modes using contact or immersion ultrasonic measurement techniques, which allow the generated longitudinal wave to strike the specimen and liquid

interface perpendicularly. Interaction $SV(\omega_1) + SV(\omega_2) \rightarrow L(\omega_1 + \omega_2)$ between two shear waves appears most promising, because it has a wave mode separation in this case. However, this interaction requires a large angle between two interacting waves (usually more than 120°), and thus it cannot be used for materials with low ultrasonic wave velocities, when a conventional immersion measurement technique is employed. Both PMMA and PVC materials used in our ageing experiments have low ultrasonic wave velocities and therefore we used the interaction $SV(\omega_1) + L(\omega_2) \rightarrow L(\omega_1 + \omega_2)$. In the epoxy cure experiments the other interaction $SV(\omega_1) + SV(\omega_2) \rightarrow L(\omega_1 + \omega_2)$ was used allowing the wave mode separation. The use of both interactions in our experiments proved their practical applicability in ultrasonic measurements. Note that both chosen interactions are the functions of just one third-order elastic constant m. Imaging and testing of the other two nonlinear elastic constants l and n require other interactions.

Measurement techniques, based on wave interactions when a nonlinear wave of difference frequency is generated, are limited to double-side-access measurement mode.

Knowing the properties of a test specimen and using the analytical results obtained in Korneev et al. [24], we have developed a procedure that enables to tune an acoustical channel for noncollinear wave mixing. For example, the tuning procedure for the through-transmission measurement case includes the following steps:

(1) Prediction of nonlinear scattering coefficients W (Eqs. (3) and (4)) for the two-plane elastic-wave interactions in an allowed or selected frequency range;
(2) Calculation of possible combinations of inclination angles θ_1 and θ_2 for the pump wave sources (Fig. 1);
(3) Evaluation of transmission coefficients $T_1(\theta_1)$ and $T_2(\theta_2)$ between a liquid and solid interface for Step 2;
(4) Calculation of nonlinear wave propagation angle α, which is a function of the θ_1 angle (angle α is between the scattered wave direction and surface normal of the test specimen);
(5) Calculation of the energy transmission coefficient $T(\alpha)$ between a solid and liquid interface for Step 4;
(6) Calculation of the amplitude function $W_T = W \times T_1 \times T_2 \times T$;
(7) Estimation of the frequency range after setting $\alpha = 0$, when the nonlinear wave strikes the solid and water interface perpendicularly.
(8) Fine tuning of θ_2 by maximization of the recorded scattered energy.

An example of calculations is shown in Fig. 2 for aluminium analyzed in [25] and PVC, when attenuation is not taken into account. The material properties are listed in Table 1. Two different noncollinear wave-mixing measurements are allowed in aluminium when an immersion ultrasonic technique is used: $SV(\omega_1) + L(\omega_2) \rightarrow L(\omega_1 + \omega_2)$ (Fig. 2a) and $SV(\omega_1) + SV(\omega_2) \rightarrow L(\omega_1 + \omega_2)$ (Fig. 3). One noncollinear wave interaction case, $SV(\omega_1) + L(\omega_2) \rightarrow L(\omega_1 + \omega_2)$, is allowed in PVC according to results obtained for aluminium when an immersion ultrasonic technique is used (Fig. 2b). It means that the conventional ultrasonic immersion technique enables to achieve conditions only for the $SV(\omega_1) + L(\omega_2) \rightarrow L(\omega_1 + \omega_2)$ interaction in PVC.

Analytical estimation of aluminium and PVC shows (Fig. 2) that a higher (by two orders) amplitude of nonlinear wave is expected in PVC. This is due to the higher nonlinearity of PVC and lower energy losses in transmissions of ultrasonic waves at water–PVC and PVC–water interfaces. First, the critical angle is seen in W_T predictions for aluminium and PVC. For the case of aluminium, the influence of the first critical angle is seen when the frequency ratio ω_2/ω_1 is 1.06. The incident angle θ_2, at which the longitudinal wave is generated in aluminium, is 12.82°, less than the first

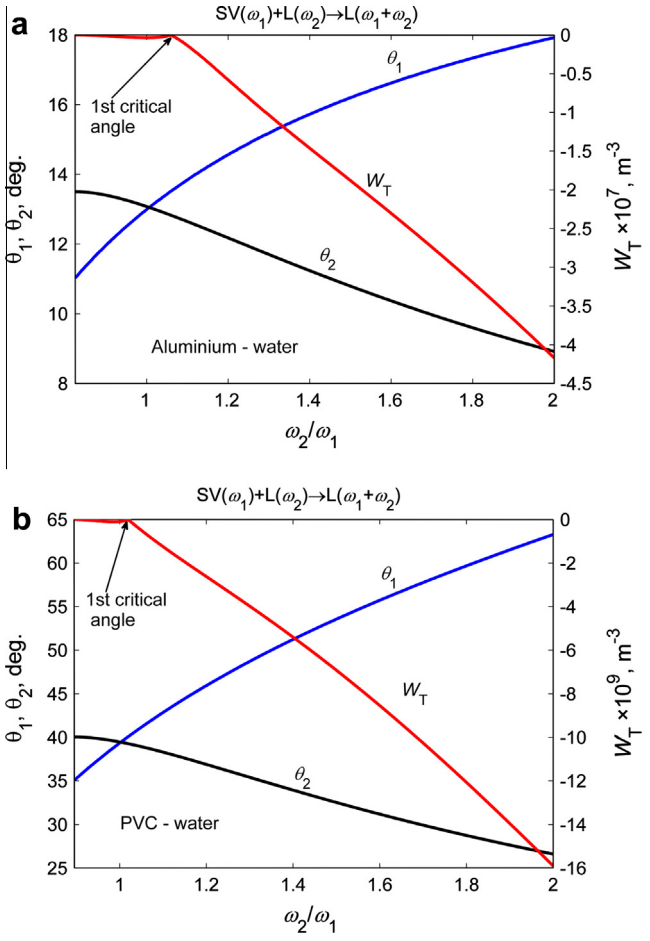

Fig. 2. Amplitude function W_T vs frequency ratio ω_2/ω_1 for $SV(\omega_1) + L(\omega_2) \rightarrow L(\omega_1 + \omega_2)$ wave mixing when the nonlinear wave strikes the specimen aluminium – water (a), and PVC – water (b) interfaces perpendicularly. Also shown are inclination angles θ_1 and θ_2 for the pump waves.

Table 1
Material properties used in the nonlinear wave analysis.

Material	λ, GPa	μ, GPa	l, GPa	m, GPa	n, GPa	ρ, kg/m^3
Aluminum	54.308	27.174	−281.5	−339	−416	2704
PVC	3.64	1.83	−33.43	−20.88	−15.86	1350

critical angle. Consequently, the ultrasonic wave energy is transmitted from water to aluminium. The incident angle θ_1 at which the shear wave is excited in aluminium is 13.52°, which corresponds to the first critical angle in the specimen. Hence, no ultrasonic shear wave energy is generated in the solids, and coefficient W_T becomes 0. When the interaction occurs between two shear waves (Fig. 3), both incident angles θ_1 and θ_2 are larger than the first critical angle, so there is no local minimum in the W_T curve.

The calculations show that for aluminium, a nonlinear wave of higher amplitude is expected in the second wave-mixing case when the frequency ratio $\omega_2/\omega_1 < 1.6$. As seen in Fig. 2a, within the calculated frequency range ($0.6 < \omega_2/\omega_1 < 2$), the highest amplitude of the nonlinear wave is expected when the frequency ratio is the highest. But it may be practically difficult to use higher frequency ratios (at MHz frequency range), because attenuation of ultrasonic waves increases with frequency, and the beam-width of resonant waves becomes very sharp. Therefore, the scattered wave will be affected by any inhomogeneity in a specimen, and especially in heterogeneous materials like rock and concrete. For

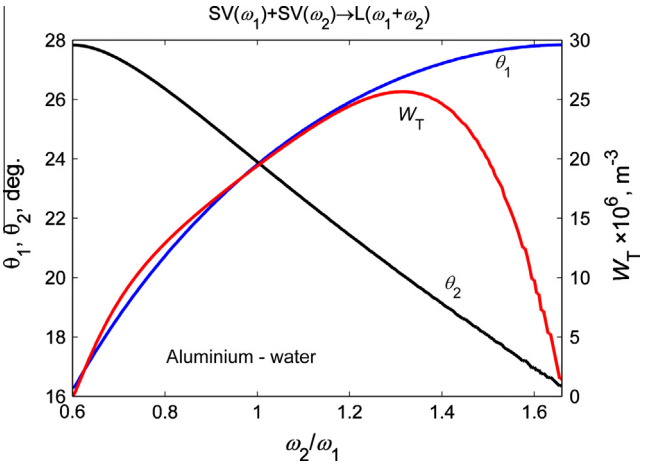

Fig. 3. Amplitude function W_T vs frequency ratio ω_2/ω_1 for $SV(\omega_1) + SV(\omega_2) \rightarrow L(\omega_1 + \omega_2)$ wave mixing in aluminium when the nonlinear wave strikes the specimen and water interface perpendicularly. Also shown are inclination angles θ_1 and θ_2 for the pump waves.

example, when the frequency of the scattered wave is 12 MHz in the aluminium specimen, the beam-width of the scattered wave, generated by an interaction volume of 5 mm radius, is less than 5° [26].

Since commercially available ultrasonic transducers of standard frequencies are available, it is practical to choose the frequency ratio of pump waves in such a way that both the performance of the transducers and the sensitivity of the receiver to the nonlinear wave stay high. With this in mind, we selected the frequency ratio ω_2/ω_1 to be 1.5, and the corresponding frequencies of the pump waves to be 6 MHz and 4 MHz, respectively. Further increase in ω_2 can be affected by a higher attenuation of the pump and nonlinear waves. A nonlinear wave of 10 MHz frequency has good separation from the 4 MHz and 6 MHz harmonics of the pump waves. Thus, the informative signal can be filtered easily from unwanted harmonics in the raw acoustic signal.

In some cases, when measurements are limited to single-side-access measurement mode, a signal-to-noise ratio can be increased employing interaction between reflections of pump waves from specimen bottom. The generated nonlinear wave will not lose energy during reflection from the specimen boundary. This option may be useful for evaluation of heterogeneous materials.

3. Measurement setup

A typical arrangement of ultrasonic transducers for immersion noncollinear wave-mixing measurements in the through-transmission mode is shown in Fig. 4. The employed geometrical parameters are listed in Table 2, with the following notation: f_1 and f_2 are the frequencies of the pump waves generated by sources S_1 and S_2, respectively. The numbers of cycles used for pump wave generation are listed in brackets after the frequencies. Inclination angles θ_1 and θ_2, as well as vertical offsets Δz_1 and Δz_2 are related to the sources S_1 and S_2 respectively. Also shown are the distance Δx between the pump wave sources, and the distance Δz between receiver R and the specimen surface. Immersion planar broadband transducers with 10 mm diameters were used for generation of the pump waves. A planar broadband sensor with a 5 MHz central frequency was used for signal reception in the physical ageing monitoring experiments. For the epoxy curing monitoring, we used a spherically focused broadband sensor with 10 MHz central frequency. The received ultrasonic signals were amplified by a 20 dB preamplifier, digitized, and stored on a personal computer

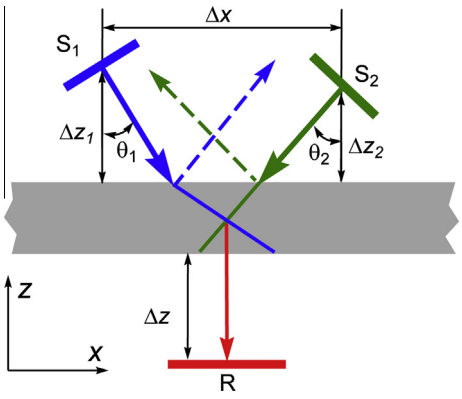

Fig. 4. Arrangement of ultrasonic transducers for the non-collinear wave mixing in the through-transmission measurement mode. Dashed lines mark the specularly reflected pump waves.

Table 2
Geometrical parameters used for the non-collinear wave mixing experiments.

Structure	f_1, MHz [cycles]	f_2, MHz [cycles]	f_r, MHz	θ_1, deg.	θ_2, deg.	Δz_1, mm	Δz_2, mm	Δz, mm	Δx, mm
PVC	2 [40]	3 [40]	5	52	31	2	19	32	35
PMMA	2 [30]	3 [50]	5	36	25	15	20.5	32	30
Al-Ep-Al	4 [30]	6 [30]	10	22	15.5	18	22	80	21

for further analysis. The received signals were filtered using a narrowband filter with a Kaiser window.

For evaluations of nonlinear wave signals we used a peak-to-peak amplitude, energy, and change of time-of-flight. In an ideal case, the peak-to-peak amplitude and energy of ultrasonic signals would give similar results, but when an ultrasonic signal has a complex wave-shape, the results may differ. Previous work has shown that for the analysis of nonlinear wave signals, it is more practical to evaluate the energy of signals [2]. When we can compare the behavior of both parameters—the peak-to-peak amplitude and energy—we present both of them.

4. Monitoring of physical ageing process in thermoplastics

For the physical ageing investigation in PMMA and PVC plates (commercially available grades), we employed the $SV(\omega_1) + L(\omega_2) \rightarrow L(\omega_1 + \omega_2)$ wave-mixing process. The plate thicknesses were 9 mm and 10 mm, respectively, and the in-plane whole specimen size was ~65 mm × 160 mm in both cases.

First, a specimen was heated in boiled water for 10 min and immediately quenched in an antifreeze liquid of temperature $T = -27$ °C. The heating was above the glass transition temperature T_g, thus erasing the previous thermo-history of the polymer. Then, the quenched specimen was placed into a water bath, where the nonlinear ultrasonic measurements were performed with a 30 s sampling rate. A magnetic stirrer was used to maintain a uniform room temperature distribution in the water bath: 18.3 ± 0.1 °C or 22.2 ± 0.2 °C for PMMA and PVC, respectively.

Fig. 5 shows typical curves sampled during the monitoring of PMMA and PVC ageing. In the beginning, when the temperature of the polymer is lower than that of water, a high nonlinear ultrasonic wave energy is measured in both polymers. An increase in the energy of the nonlinear wave simultaneous with a decrease in temperature was reported [2]. During the experiment, the specimen temperature increases because of the heat exchange. Therefore, the energy of the nonlinear ultrasonic wave decreases, with this trend ending when the specimen temperature becomes equal

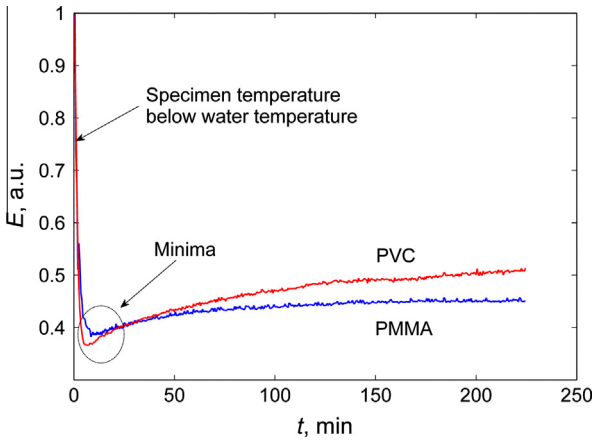

Fig. 5. Measured nonlinear wave energy evolution during physical ageing process in PMMA and PVC. Minima location shows when the specimen and water temperatures become equivalent.

to that of water. This temperature equilibrium is seen in Fig. 5, when the energy of the nonlinear wave becomes lowest, which was observed after about 9 min and 7.5 min for PMMA and PVC, respectively. Further, the nonlinear wave energy starts to increase due to the physical ageing in the polymers. The highest energy-increase ratio is observed between 9 min and 100 min, signifying that the ageing rate is also the highest in this range. As time progresses, the ageing slows down, especially for PMMA.

Typically, the physical ageing process is presented in a logarithmic time scale, as is done in Fig. 6. This figure shows the relative changes in the energy of nonlinear waves $\Delta E = (E - E_0)/E_0 \times 100\%$, where E_0 is the minimal measured magnitude (see Fig. 5). The curves show that the ageing is faster in PMMA than in PVC—in agreement with the reported results in [27].

The test curves (Figs. 5 and 6) show that the ageing process is relatively complete for PMMA after about two hours, because the energy of the nonlinear wave increases very slowly after this time. This is not as apparent in Fig. 6, because of the logarithmic scale. The shape of the measured curve for PMMA corresponds closely to the theoretical shape-reported in [4], where it is shown that the parametric curve obtains a sigmoidal shape. Knowing that temperature accelerates physical ageing (and despite the fact that the temperature was 4 °C higher than for PMMA), we observed that in the PVC specimen, the ageing process was not completed in the same time window as in the PMMA specimen.

To illustrate the physical ageing influence on material properties, additional measurements were performed for the PMMA and PVC specimens. Each specimen was prepared as follows: One half of the plate was isolated from both sides, to protect the specimens from heating as much as possible. After that, the uncovered part was immersed in boiling water for 10 min, to rejuvenate the material locally. Finally, the entire specimen was immediately quenched in an antifreeze liquid at a temperature $T = -27$ °C. Then the specimens were scanned using linear and nonlinear ultrasonics with a 1 mm step, along a central line. The linear scanning was performed using a 5 MHz broadband transducer in a pulse-echo mode employing single-pulse excitation.

Scanning results for the PMMA plate are presented in Fig. 7. The figure clearly shows a high nonlinear wave energy difference between the rejuvenated and unprocessed zones. In the measured energy of the nonlinear wave, a transient zone is observed between both the rejuvenated and nonrejuvenated plate parts. Obviously, this transient zone was affected by water vapor as well as by heat conduction from the immersed part. At the same time, the linear ultrasonic measurement of the peak-to-peak amplitude shows very little sensitivity to the physical ageing of PMMA. Moreover, the transient zone is not seen in this data. A small linear trend, seen in the linear measurements of time-of-flight, could be caused by a specimen misalignment; and it is clearly seen that there is no correlation between the nonlinear wave signal and the time-of-flight of the linear ultrasonic signals.

The ultrasonic scans for the PVC plate are shown in Fig. 8. The nonlinear wave energy exhibits a pronounced difference (relative change is up to 230%) between rejuvenated and nonrejuvenated zones. This difference could be caused not only by physical ageing, but also by the effects of ageing combined with thermal expansion. Mechanical measurements of plate thickness and ultrasonic measurements of the time-of-flight for ultrasonic waves confirmed that plate thickness increased locally by about 0.1 mm after heating in the boiling water. This conforms with test data for thermal expansion reported in [27], which show that heating above ≈75 °C results in a drastic (and probably partially irreversible) "jump" in PVC volume, whereas the thermal expansion of PMMA is still relatively low. Thus, we believe that the linear ultrasonics detected different zones in the PVC not because of its sensitivity to material properties, but due to thermal expansion and probable water absorption—in accord with previous studies [1,28], which demonstrated that the linear ultrasonics is insensitive to the physical ageing of PVC.

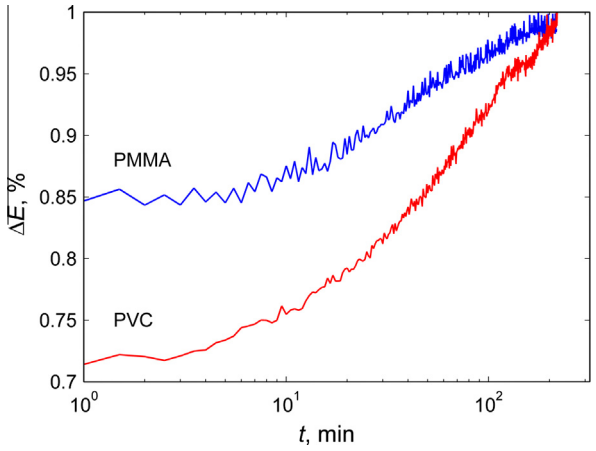

Fig. 6. Measured dynamics of the physical ageing processes in PMMA and PVC.

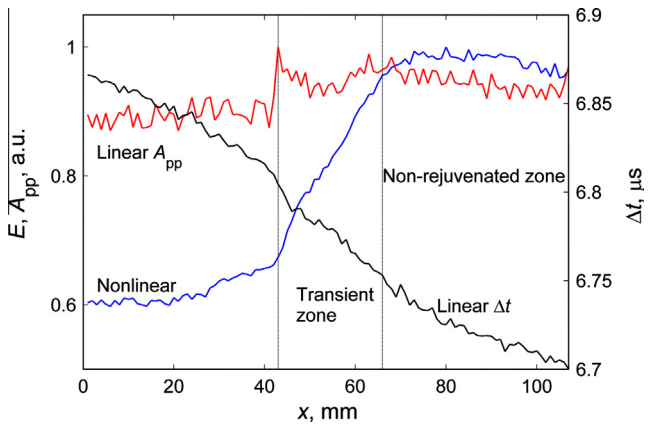

Fig. 7. Measured physical ageing state in PMMA plate using nonlinear and linear ultrasonics; one central line was scanned along the specimen.

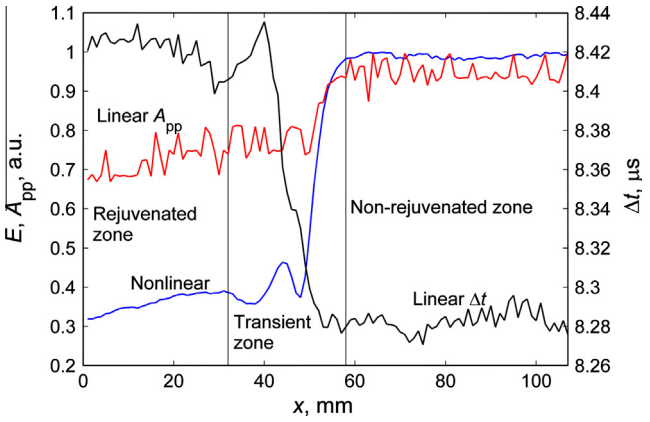

Fig. 8. Physical ageing state in PVC plate using nonlinear and linear ultrasonics.

5. Monitoring of epoxy curing

Epoxy curing processes are well studied with linear ultrasonic measurement techniques (for example, see reported works [6–8,29–33]). The linear ultrasonic technique is shown to be applicable for monitoring of thin (about 0.5 mm) epoxy layers [33] and for detection of the gelation time (when a viscous liquid transforms into an elastic gel) [31,32,34]. However, there is insufficient information about detection of the vitrification time (when the mobility of reactive groups vanishes) [35]. In this section, we present a nonlinear ultrasonic measurement technique that enables us to monitor epoxy curing in a thin layer, with robust detection of the typical points (gelation and vitrification). A verification and explanation of the ultrasonic measurement results are presented in the next section.

To monitor isothermal epoxy curing, we used the $SV(\omega_1) + SV(\omega_2) \rightarrow L(\omega_1 + \omega_2)$ wave-mixing process. The epoxy we employed was a typical commercial system comprising 3/4 of Araldite® LY1564SP resin and 1/4 of XB3486 hardener, by mass [36]. The components were degassed for 20 min after mixing, and then the mix was directly (with only a 5–10 min delay) used for the tests. In the rheometry tests reported in the next section, the preparations required more time, and the delay was about 20 min.

The prepared epoxy was spread on a 4 mm thick aluminium plate and then covered by a second identical aluminium plate. (To provide a uniform thickness for the epoxy layer, a 0.2 mm thick double-sided tape was placed to form a 1 cm wide barrier on the sides of the plate). Then, the aluminium plates were fixed (using bolts) and sealed (using a tacky "gum") to isolate the epoxy from water. Finally, the specimen was placed in a water bath under an acoustic channel adjusted for mixing the ultrasonic waves in a single 4 mm thick aluminium plate.

Arrangement of the ultrasonic transducers and specimen was chosen in such a way that the central beams of pump waves would intersect in the epoxy layer. Because of this arrangement and finite beam width (which was of the same order as the pump wave-transducer diameters), the following three volumes (where the nonlinear wave interactions occurred) could be separated:

(1) Volume 1 in the upper aluminium layer. The interaction of pump waves occurred without the influence of epoxy. Consequently, a constant amount of nonlinear wave energy was generated.
(2) Volume 2 in the epoxy layer. The nonlinear wave was either not generated or very poorly generated, because the wave-interaction conditions for aluminium were chosen.
(3) Volume 3 in the lower layer of aluminium. The resulting amount of nonlinear wave energy in this volume was expected to be strongly dependent on the epoxy-layer properties. Because of changes in the longitudinal and shear-wave velocities during epoxy curing, transmission and refraction of ultrasonic waves varied between the epoxy and aluminium interfaces. Hence, the synchronistic conditions of wave interaction were not completely fulfilled (i.e., generation of the nonlinear wave was ineffective). Moreover, these conditions varied, owing to changes in the acoustic properties of epoxy. Therefore, the amount of the generated wave energy varied considerably in this volume.

Monitoring of the curing process was performed at 24.3 °C or at 40 °C with a 30 s sampling rate. Three parameters of the nonlinear ultrasonic wave were analyzed: the peak-to-peak amplitude, energy, and group time-of-flight of signal. The time-of-flight for the nonlinear signal was determined using the first measurement signal as the reference.

Test data for the 24.3 °C case are presented in Fig. 9a; they clearly show three typical points, seen at 1.3 h, 6.7 h (10 h) and 20 h. The first peak at 1.3 h is well indicated by all three parameters. The measured minimum at 6.7 h is clearly indicated by the nonlinear wave peak-to-peak amplitude and energy. However, in the time-of-flight curve, this peak has shifted further and is situated at about 10 h. Fig. 9 shows that a small deviation occurred (different slopes) between the peak-to-peak amplitude and energy curves within the time interval 10–20 h. The third typical point (at about 20 h) is not easily determined in the curves, but the time-of-flight curve has a clear change of phase at this point. The measured

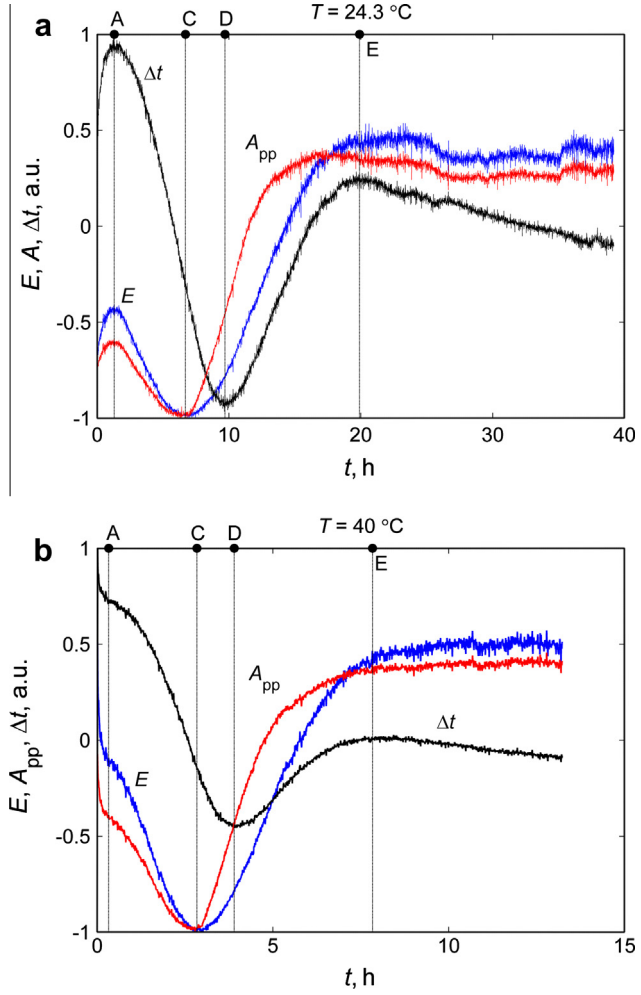

Fig. 9. Dynamics of the nonlinear ultrasonic signal parameters during epoxy curing at 24.3 °C (a) and 40 °C (b). The parameters are scaled by their maxima and centred.

energy and peak-to-peak amplitude tend to become constant after passing this point.

Fig. 10 shows typical nonlinear ultrasonic signals at the characteristic points discussed above. The signals are scaled by the maximum amplitude of the signal measured at 20 h. We see here that the informative signal duration becomes shorter during the curing process, which indicates solidification of the epoxy.

Test data for the 40 °C case are presented in Fig. 9b. Clearly, the curing process has been accelerated by the higher temperature in comparison with the 24.3 °C case. The initial linear decrease in energy and amplitude was caused by the lower initial temperature of the specimen. These results agree very well with the measurement results for physical ageing in PMMA and PVC (see Fig. 5). The following characteristic points can be derived from Fig. 9b: 0.3 h, 2.8 h (3.9 h) and 7.8 h. However, the first point (0.3 h) is not so well pronounced in this measurement as before for the 24.3 °C case. This point is now seen only indirectly, as a local inflection of the curves.

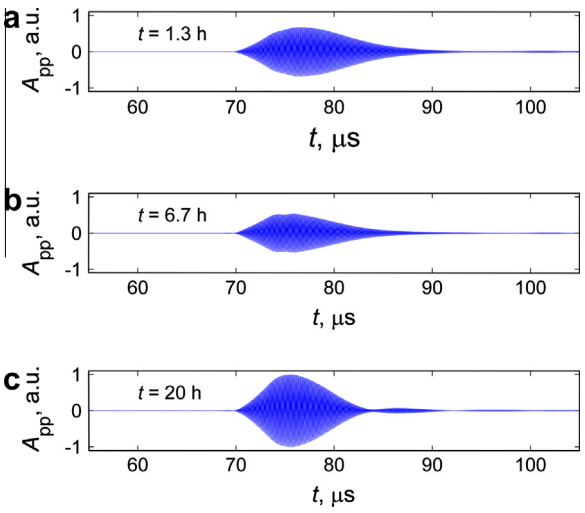

Fig. 10. Typical nonlinear ultrasonic signals during epoxy curing at 24.3 °C: minimum viscosity point (a), gelation point (b) and vitrification point (c).

Note that these ultrasonic measurements were performed in a large water bath, without a forced control of temperature, which changed slightly during the day-night cycle. This change caused small "jumps" in the curves, seen, for example, in Fig. 9a between 25 h and 37 h.

6. Verification of epoxy curing by rheometry

An alternative cure characterization was performed using an Anton Paar®MCR501 parallel plate rheometer. This test method is widely used for this purpose (for example, see [37]), and its results can easily be interpreted in rheologic terms (viscosity, damping, etc.).

First, a 26 mm diameter ring was mounted on the bottom plate and partially filled with a 3–4 mm epoxy layer. Then, a 25 mm diameter top plate was sunk into this ring until it contacted the epoxy. After closing the chamber and setting the gained temperature, the shear viscosity was measured at a 1 Hz frequency and a 1.8° amplitude of rotational oscillations.

Results for 25 °C are shown in Figs. 11 and 12, while Fig. 13 shows results for the 40 °C case. Fig. 12 depicts a zoomed part of Fig. 11, showing details of the low-signal behavior (similar curves are not shown for 40 °C case from Fig. 13, since no local changes are seen in the quite smooth curves). The following characteristic points can be observed in these figures, enabling a better understanding of their physical backgrounds:

(1) The first extremum, point A, corresponds to the minimum viscosity, which obviously occurs not directly after mixing of the resin and hardener, but (due to inertia in the chemical processes) is postponed for some time: about 2 h at 25 °C. This effect is not visible in the 40 °C test conditions; in the 25 °C case, it roughly corresponds to 1.3 h, noted above when discussing Fig. 9a.

(2) After a while, at point B, ~4 h at 25 °C, the reaction rate increases. This is seen as a minor local maximum of viscosity or a minor local minimum of the damping factor (then it starts to grow rapidly), and the onset of the loss modulus growth, again for the 25 °C case only. Point B is not detected for the 40 °C case, likely owing to the absence of any reaction-rate change in this case.

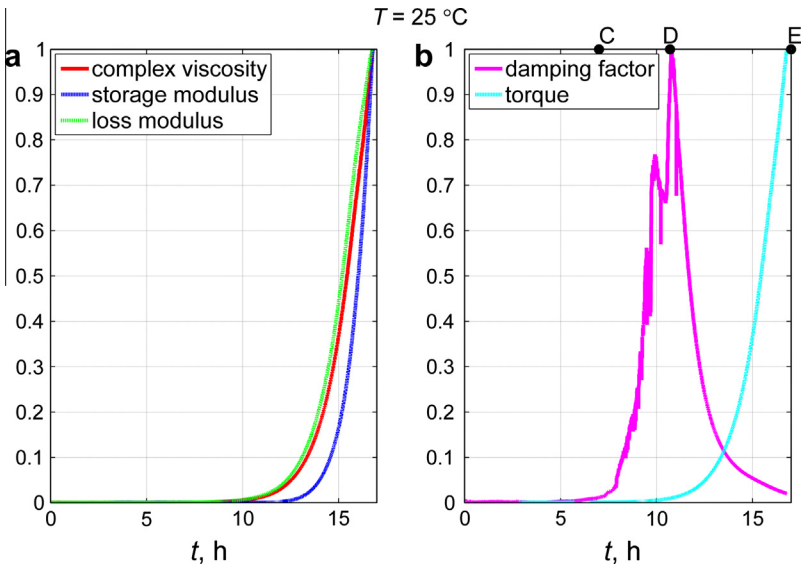

Fig. 11. Cure monitoring using rheometry, 25 °C case.

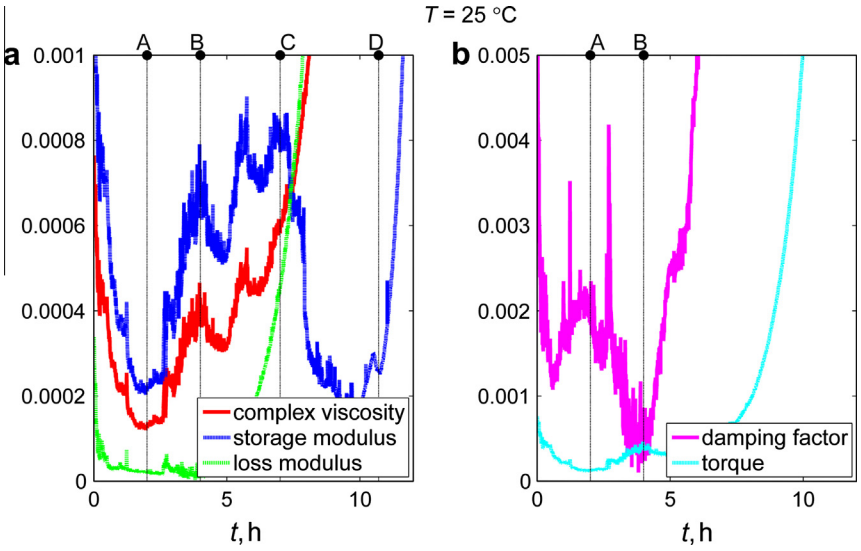

Fig. 12. Cure monitoring using rheometry, 25 °C case (zoomed).

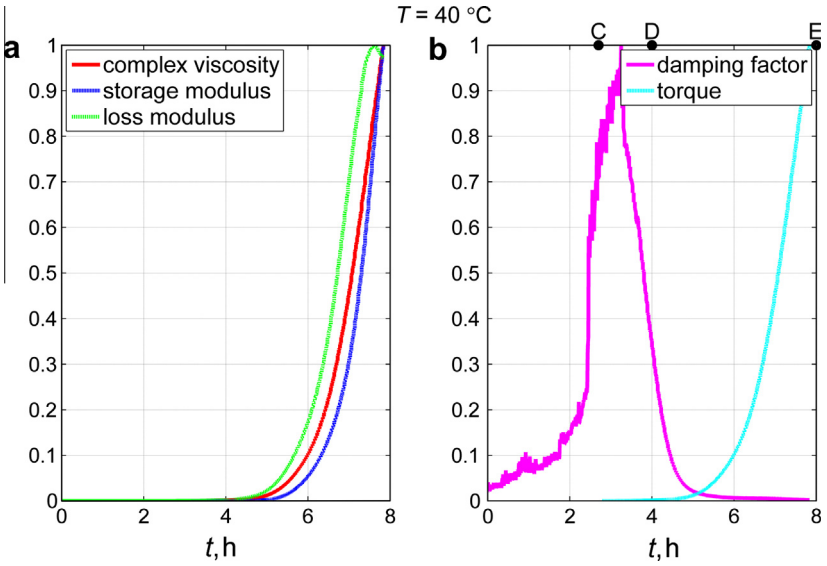

Fig. 13. Cure monitoring using rheometry, 40 °C case.

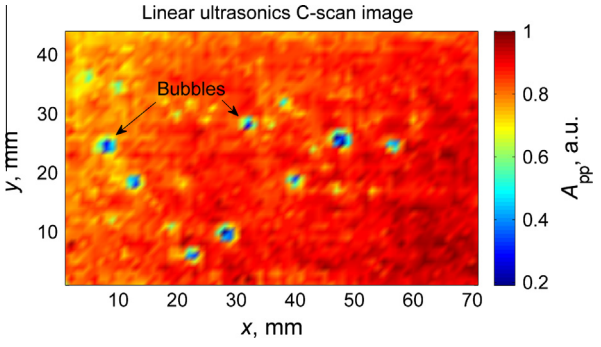

Fig. 14. Amplitude C-scan image, by the linear ultrasonic measurement.

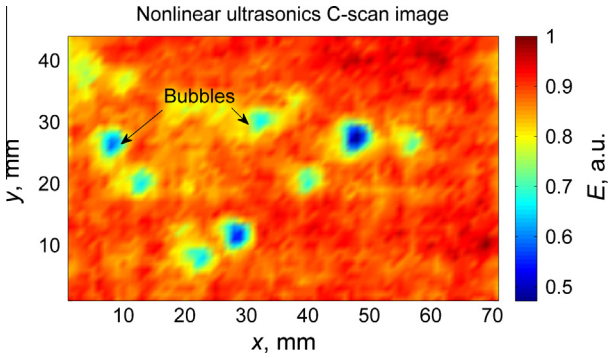

Fig. 15. Energy C-scan image, by the nonlinear ultrasonic measurement.

(3) The following extremum, point C, is the onset of gelation; it occurs at about 7 h at 25 °C or 2.7 h at 40 °C. At this moment, the storage modulus reaches its local maximum, and the damping-factor rate becomes yet higher. This feature corresponds well to the 6.7 h and 2.8 h points noted above when discussing Fig. 9.

(4) The next extremum, point D, occurring at about 10–11 h at 25 °C or 4 h at 40 °C, is the peak of gelation and, therefore, of the damping factor as well. Afterwards, the damping ability of the material vanishes rapidly. All other rheometry variables start to increase in magnitude, also very rapidly. Point D is also visible in Fig. 9 (10 h or 3.9 h estimated for 25 °C and 40 °C cases, respectively).
(5) The last extremum is the onset of vitrification, point E, at about 17 h for 25 °C or 8 h for 40 °C. The rheometry is automatically stopped at this stage, due to exceeding the allowable torsional moment. When the specimens are then taken out of the machine, they appear completely solidified. This final point also agrees well with the vitrification times derived from Fig. 9 (roughly 20 h or 7.8 h, respectively).

7. C-scanning experiments

The key issue of this research is the comparison of the linear and nonlinear ultrasonic measurement techniques with application to a non-destructive evaluation in a three-layered structure. Currently, there is too little information about those investigations in which nonlinear and immersion-ultrasonic-measurement techniques are used.

To approach this, we used two 4 mm thick aluminium plates bonded with the same epoxy resin. When the epoxy cure was completed at room temperature, the specimen was placed in a water bath, and C-scanning was performed at 1 mm steps in x and y directions, using both linear and nonlinear ultrasonic techniques. The linear pulse-echo measurements employed a spherically focused 10 MHz transducer. The nonlinear scanning was performed using the same arrangement of ultrasonic transducers as in the epoxy cure monitoring discussed above, i.e. employing the interaction $SV(\omega_1) + SV(\omega_2) \rightarrow L(\omega_1 + \omega_2)$.

A peak-to-peak amplitude C-scan image, given by the linear ultrasonic measurement, is presented in Fig. 14. The nonlinear ultrasonic results are presented in Fig. 15 for the same specimen. Bubbles (naturally appearing during the epoxy cure) are seen as the low-amplitude spots (Figs. 14 and 15). The bubbles are not as prominent in the nonlinear ultrasonics C-scan image in comparison with Fig. 14. This can be explained by a better focused beam during the pulse-echo scanning. Actually, an elongation of inhomogeneity dimensions during the nonlinear ultrasonics scanning is similar to situation when Lamb waves are used to visualize the imperfections [38]. Therefore, forming of high resolution ultrasonic images (with a resolution of a few millimetres or parts of millimetre) can be complicated using the noncollinear wave mixing technique.

8. Conclusions

Nonlinear immersion ultrasonic-measurement techniques are presented in this study, with applications for monitoring the material transformations in polymers. We demonstrate that the nonlinear ultrasonics, based on noncollinear wave mixing, can be very sensitive to small changes in materials—changes that are hardly detectible (or undetectable) using linear ultrasonic-measurement techniques. The nonlinear technique can be used for contactless *in situ* monitoring of dynamic material properties, as well as for non-destructive testing.

The most remarkable results are obtained for the physical ageing processes in thermoplastics (PMMA and PVC). The ageing is well detected by the nonlinear ultrasonic technique, while the linear technique is insensitive to physical ageing. For example, the nonlinear data for PMMA show a 40% difference between zones of "young" and "aged" material, whereas the linear data show no difference at all. For PVC, while the linear ultrasonics indicates a 45% difference (presumably caused by an irreversible thermal expansion of the material), the nonlinear ultrasonics shows as much as a 230% difference.

The nonlinear ultrasonic method is also shown to effectively detect the main characteristics of the epoxy cure process: the time of maximal viscosity, the gel time, and the vitrification time. These results agree closely with those obtained using a conventional parallel-plate DMA method.

Finally, a simple test demonstrates the ability of the nonlinear ultrasonic technique for a non-destructive testing with results comparable with the linear ultrasonic technique. However, the nonlinear technique seems to provide a lower spatial resolution to imperfections in the specimen geometry. (This disadvantage can be minimized by using more dedicated pump wave sources).

Possible advantages offered by the presented nonlinear ultrasonic technique include: (a) the wave-mode and frequency separations, (b) elimination of surrounding medium influence, (c) steering (scanning) the scattered wave and controlling the intersection volume location, (d) single or double-sided measurements, and (e) operating in the detector mode (for example, no informative signal excitation until the material properties are homogenous).

Acknowledgments

This work was performed partially in collaboration with Vitens and ApplusRTD, within the 'Innowator' project IWA-08019, as funded by the Dutch Ministry of Economic Affairs by means of Agentschap NL. This support is gratefully acknowledged. This work was also supported by the Director, Office of Energy Research, Office of Basic Energy Sciences, Chemical Sciences, Geosciences, and Biosciences Division, of the U.S. Department of Energy under Contract No. DE-AC02-05CH11231.

References

[1] A. Demčenko, R. Akkerman, P.B. Nagy, R. Loendersloot, Non-collinear wave mixing for non-linear ultrasonic detection of physical ageing in PVC, NDT & E Int. 49 (2012) 34–39.
[2] A. Demčenko, M. Ravanan, H. A. Visser, R. Loendersloot, R. Akkerman, Investigation of PVC physical ageing in field test specimens using ultrasonic and dielectric measurements, in Proceedings of the IEEE International Ultrasonics Symposium, (2012) 1909-1912.
[3] A. Demčenko, Non-collinear wave mixing for a bulk wave phase velocity measurement in an isotropic solid, in Proceedings of the IEEE International Ultrasonics Symposium, (2012) 1437–1440.
[4] K. Chen, K.S. Schweizer, Theory of physical aging in polymer glasses, Phys. Rev. E 78 (2008). 031802–1–031802–15.
[5] K. Chen, K.S. Schweizer, Molecular theory of physical aging in polymer glasses, Phys. Rev. Lett. 98 (2007) 167802.
[6] W.P. Winfree, Ultrasonic characterization of changes in viscoelastic properties during cure, IEEE Ultrason. Symp. Proc. 1 (1983) 866–869.
[7] R.J. Freemantle, R.E. Challis, Combined compression and shear wave ultrasonic measurements on curing adhesive, Meas. Sci. Technol. 9 (1998) 1291–1302.
[8] S. Dixon, D. Jaques, S.B. Palmer, G. Rowlands, The measurement of shear and compression waves in curing epoxy adhesives using ultrasonic reflection and transmission techniques simultaneously, Meas. Sci. Technol. 15 (2004) 939–947.
[9] M.A. Breazeale, D.O. Thompson, Finite-amplitude ultrasonic waves in aluminum, Appl. Phys. Lett. 3 (5) (1963) 77–78.
[10] P.H. Carr, Harmonic generation of microwave phonons in quartz, Phys. Rev. Lett. 13 (10) (1964) 332–335.
[11] P.H. Carr, Harmonic generation of microwave phonons by radiation pressure and by the phonon-phonon interaction, IEEE T. Son. Ultrason. 13 (3) (1966) 103–108.
[12] K.K. Ermilin, L.K. Zarembo, V.A. Krasil'nikov, Generation of superhigh frequency acoustic harmonics in a lithium niobate crystals, Sov. Phys. Solid State 12 (1970) 1045–1052.
[13] A.A. Gedroits, V.A. Krasil'nikov, Finite-amplitude elastic waves amplitude in solids and deviations from the Hook's law, JETP Lett. 16 (1963) 1122.
[14] P.A. Johnson, K.R. McCall, Observation and implications of nonlinear elastic wave response in rock, Geophys. Res. Lett. 21 (3) (1994) 165–168.
[15] Y. Hiki, K. Mukai, Ultrasonic three-phonon process in copper crystal, J. Phys. Soc. Jpn. 34 (2) (1973) 454–461.

[16] F.R. Rollins, L.H. Taylor, P.H. Todd, Ultrasonic study of three-phonon interactions. II. Experimental results, Phys. Rev. 136 (3(A)) (1964) A597–A601.
[17] L.K. Zarembo, V.A. Krasil'nikov, Nonlinear phenomena in the propagation of elastic waves in solids, Sov. Phys. Usp. 13 (6) (1971) 778–797.
[18] P.A. Johnson, T.J. Shankland, R.J. O'Connell, J.N. Albright, Nonlinear generation of elastic waves in crystalline rock, J. Geophys. Res. 92 (5(B)) (1987) 3597–3602.
[19] P.A. Johnson, T.J. Shankland, Nonlinear generation of elastic waves in granite and sandstone: continuous wave and travel time observations, J. Geophys. Res. 94 (B12) (1989) 17,729–17,733.
[20] H.H. Barrett, J.H. Matsinger, Interaction of almost-collinear longitudinal phonons, Phys. Rev. 154 (3) (1967) 877–886.
[21] R.W. Dunham, H.B. Huntington, Ultrasonic beam mixing as a measure of the nonlinear parameters of fused silica and single-crystal NaCl, Phys. Rev. B 2 (4) (1970) 1098–1107.
[22] A.J. Croxford, P.D. Wilcox, B.W. Drinkwater, P.B. Nagy, The use of non-collinear mixing for nonlinear ultrasonic detection of plasticity and fatigue, J. Acoust. Soc. Am. 126 (5) (2009) EL117–EL122.
[23] F.D. Murnaghan, Finite Deformation of Elastic Solid, John Wiley, New York, 1951.
[24] V.A. Korneev, K.T. Nihei, L.R. Myer, Nonlinear interaction of plane elastic waves, Tech. Rep. LBNL-41914, Lawrence Berkeley National Laboratory, USA, 1998.
[25] J.R. Asay, A.H. Guenther, Ultrasonic studies of 1060 and 6061–T6 aluminum, J. Appl. Phys. 38 (10) (1967) 4086–4088.
[26] I.A. Beresnev, Interaction of two spherical elastic waves in a nonlinear five-constant medium, J. Acoust. Soc. Am. 94 (6) (1993) 340–3404.
[27] R. Greiner, F.R. Schwarzl, Thermal contraction and volume relaxation of amorphous polymers, Rheol. Acta 23 (4) (1984) 378–395.
[28] B.E. Read, G.D. Dean, P.E. Tomlins, J.L. Lesniarek-Hamid, Physical ageing and creep in PVC, Polymer 33 (13) (1992) 2689–2698.
[29] A.M. Lindrose, Ultrasonic wave and moduli changes in a curing epoxy resin – Ultrasonic techniques are examined as a means for monitoring reaction extent and the development of solid-phase moduli in a curing epoxy, Exp. Mech. 18 (6) (1978) 227–232.
[30] S.I. Rokhlin, D.K. Lewis, K.F. Graff, L. Adler, Real-time study of frequency dependence of attenuation and velocity of ultrasonic waves during the curing reaction of epoxy resin, J. Acoust. Soc. Am. 79 (6) (1986) 1786–1793.
[31] I. Alig, K. Nancke, G.P. Johari, Relaxations in thermosets. XXVI. Ultrasonic studies of the temperature dependence of curing kinetics of diglycidyl ether of bisphenol-A with catalyst, J. Polym. Sci. Part B: Polym. Phys. 32 (8) (1994) 1465–1474.
[32] M. Matsukawa, I. Nagai, Ultrasonic characterization of a polymerizing epoxy resin with imbalanced stoichiometry, J. Acoust. Soc. Am. 99 (4) (1996) 2110–2115.
[33] S. Dixon, C. Edwards, S.B. Palmer, A technique for accurate shear wave velocity measurements of thin epoxy resin samples using electromagnetic acoustic transducers (EMATs), Meas. Sci. Technol. 12 (5) (2001) 615–621.
[34] J.C. Bacri, J.M. Courdille, J. Dumas, R. Rajaonarison, Ultrasonic waves: a tool for gelation process measurements, J. Phys. Lett.-Paris 41 (15) (1980) 369–372.
[35] C.Y. Shigue, R.G.S. Dos Santos, C.A. Baldan, E. Ruppert-Filho, Monitoring the epoxy curing by the dielectric thermal analysis method, IEEE T. Appl. Supercon. 14 (2) (2004) 1173–1176.
[36] Warm-curing epoxy system based on Araldite® LY 1564 SP/Hardener XB3486/Hardener XB3487. Huntsman datasheet, (2004).
[37] D.J. O'Brien, P.T. Mather, S.R. White, Viscoelastic properties of an epoxy resin during cure, J. Compos. Mat. 35 (10) (2001) 883–904.
[38] A. Demčenko, E. Žukauskas, R. Kažys, A. Voleišis, Interaction of the A0 lamb wave mode with a de-lamination type defect in GLARE3-3/2 composite material, Acta Acust. United AC 92 (4) (2006) 540–548.